INVESTIGATION OF THE EFFECT OF BEAM SPACE-CHARGE ON ELECTRON TRAJECTORIES IN IONIZATION PROFILE MONITORS

D. Vilsmeier, B. Dehning, M. Sapinski, CERN, Geneva, Switzerland

Abstract

The correct measurement of beam size using an ionization profile monitor relies on the confinement of electron trajectories from their source to the electron-sensitive detector. This confinement is provided by a magnetic field aligned with electric extraction field. As the initial electron velocities are boosted by the presence of a high-charge density beam, the value of the magnetic field depends on both the beam size and on the charge density. If the magnetic field is not strong enough a deformation of the observed beam profile occurs. In this paper the results of a study of electron trajectories in the presence of high charge density beams is presented along with an estimation of the required magnetic field for various scenarios. A correction procedure for compensating any residual distortions in the measured profile is also discussed.

INTRODUCTION

During the calibration procedure of the LHC Ionization Profile Monitor (IPM) [1] it has been found that the obtained profiles at high beam energy are broader than expected [2, 3]. Several reasons for this effect have been investigated:

- wrong correction for camera tilt with respect to the beam direction,
- optical point-spread-function (PSF),
- PSF due to multi-channel plate granularity,
- underestimation of electron gyroradius.

Finally the problem was tracked down to the beam space charge which kicks electrons before they leave the beam, significantly increasing their gyroradius. An increase of the magnetic field was suggested, however it is a costly solution. In this paper the details of the interaction of electrons with the beam field are investigated and numerical methods to correct the profiles are suggested.

In order to simulate the beam space charge impact on electron trajectories a modified version of PyECLOUD [4] code is used. PyECLOUD is a 2D tracking code which does not take into account the longitudinal electric field nor the magnetic field of the bunches. Both limitations are a good approximation for high-relativistic beams interacting with slowly-moving electrons. The external fields in the simulation are perfectly aligned and uniform. The beam optics functions in the monitor are assumed to be: β_x = 213 m, β_y = 217 m (corresponding to vertical device on beam 2) and dispersion is zero. The emittance has the same value in horizontal and vertical plane. Table 1 shows beam parameters of cases analyzed in detail.

Table 1: Simulated Cases Studied in Detail

parameter	450 GeV	4 TeV	6.5 TeV
emittance [μm]	1.7	2.4	1.7
bunch			
-intensity [$\cdot 10^{11}$]	1.5	1.7	1.3
-length [ns]	1.2	1.2	1.25
σ_{beam} [μm]	869	346	229

In addition three cases of beam energy ramps are considered, for beams with normalized emittance ϵ_n = 1.5 μm, bunch length of 1.1 ns and bunch charge of $N_b = 1.1 \cdot 10^{11}$, $1.3 \cdot 10^{11}$ and $1.5 \cdot 10^{11}$ protons. Fifteen beam energies between 450 GeV and 7 TeV are simulated in each case. The simulated bunches are gaussian in transverse and longitudinal directions.

In the following we describe the initial velocity distribution of electrons and effects of space charge on profile shape and the gyroradius. In the end we discuss the corrections for the observed distortions of the beam profiles.

INITIAL VELOCITIES

In the previous work it has been estimated that the distribution of initial velocities of electrons plays an important role in the shape of the beam profile observed in IPM (see Fig. 4.5 in [5]). This distribution was obtained using Geant4 program and turned out to be significantly overestimated. Here the generation of initial velocities is based on an analytic model [6].

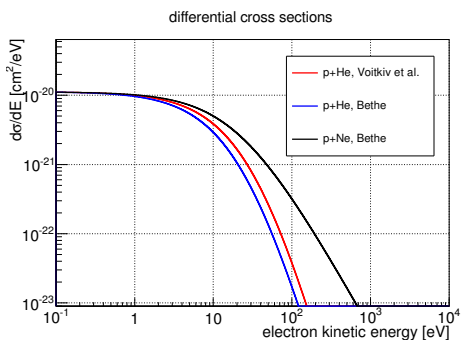

Figure 1: Example of cross-sections calculated with Bethe [7] approximation and a more accurate [6] model for 4 TeV protons.

The main contribution to the ionization process is due to electric dipole interaction between the projectile and the target electron. Most of the interactions are associated with small momentum transfer and the produced electrons are soft.

ISBN 978-3-95450-173-1

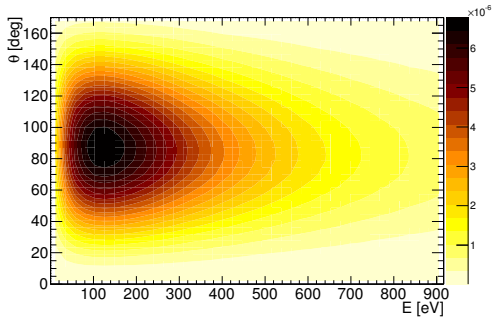

Figure 2: Double differential cross section [6]. Electrons are emitted transversely to the beam direction.

Figure 1 presents the comparison of distributions of the kinetic energy of electrons produced in proton interactions with helium and neon gases. The used approximation neglects forward processes (for instance binary peak) which have negligible contribution for relativistic projectiles.

The gyrofrequency of the circular component of electron motion is about 35.1 GHz. The time in which electrons reach the detector is about 3.2 ns and the number of revolutions is around 100.

BUNCH FIELD

The magnitude of the electric fields inside the atom is about $5 \cdot 10^{11}$ V/m. The IPM extraction field is about $5 \cdot 10^{4}$ V/m. The field inside the bunch is shown in Fig. 3. For the case of 6.5 TeV beam it reaches $E^{max}_{bunch} = 8 \cdot 10^{5}$ V/m. The scalar polarizability of neon atoms is about $4.41 \cdot 10^{-41} C^2 m^2 J^{-1}$, therefore the Stark effect due to bunch field leads to a negligible shift of atomic levels and does not affect the ionization potential.

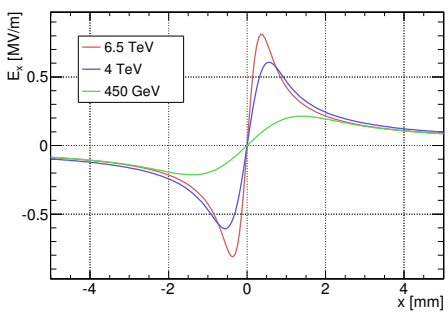

Figure 3: The radial component of the electric field as a function of distance from the bunch center for the three cases from Table 1.

EFFECT OF SPACE CHARGE ON PROFILES

The observed deformation of the beam profile is non-gaussian and depends on the local charge density inside the bunch. In Fig. 4 the initial (original) and deformed (final) profiles are shown. The profiles become more peaked then gaussian and with larger tails. One way to measure non-gaussianity of the obtained distribution is squared kurtosis. Kurtosis is zero for gaussian and becomes positive if the peak of the distribution is spikier then gaussian[1].

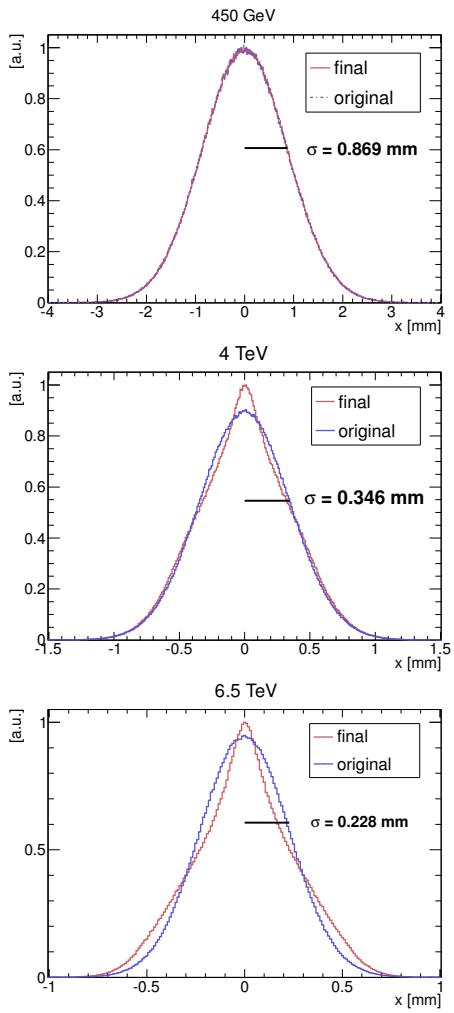

Figure 4: Deformation of the profile for the three cases from Table 1. The blue lines are original beam profiles while red ones are profiles registered by the IPM, deformed due to beam space charge.

Figure 5 shows the squared kurtosis for profiles obtained from various beams (ramp cases). For beam sizes below 0.3 mm an increase of the kurtosis is observed. Similar behaviour is observed when trying to fit gaussian (using ROOT [8] fit procedure) to the distorted profile. The non-gaussianity of the profiles becomes strong for the beam sizes corresponding to energies of about 3-4 TeV.

A lot of functions have been tested trying to find the best description of the distorted profiles. One of the best candidates is a combination of Gauss and Laplace functions:

[1] Kurtosis is sensitive to outliers but this is not important for the simulation study, however for real data analysis another way to quantify non-gaussianity, for instance differential entropy, should be used.

ISBN 978-3-95450-173-1

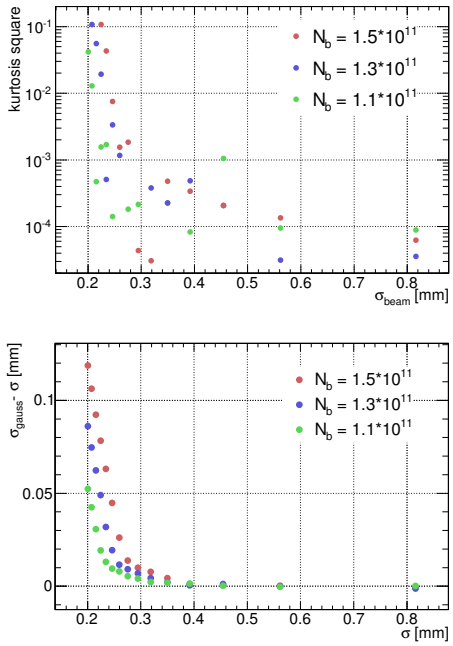

Figure 5: Non-gaussianity for various beams. Upper plot: kurtosis as a function of the original beam size, bottom one: difference between fitted and original gaussian.

$$f(x) = p_0 \cdot \exp\left(-\frac{x^2}{2\sigma_g^2}\right) + p_1 \cdot \exp\left(-\frac{|x|}{\sigma_l}\right) + p_2 \qquad (1)$$

Using this 5-parameter function nearly every profile could be fitted - see for example Fig. 6. Unfortunately no simple correlation has been found between the original profile width (σ_{beam}) and fit parameters ($p_0, p_1, \sigma_g, \sigma_l$).

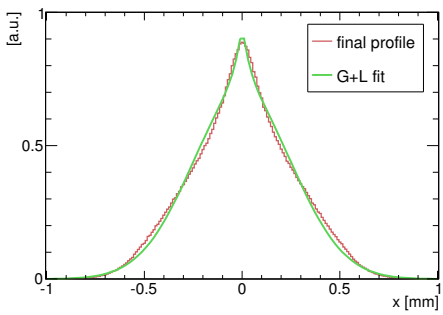

Figure 6: Results of fitting the distorted profile at 6.5 TeV with function 1.

EFFECT OF SPACE CHARGE ON GYRORADIUS

The simulations show that the effect driving the profile distortion is a dramatic increase of gyroradii. The gyration center is also shifted with respect to the production point,

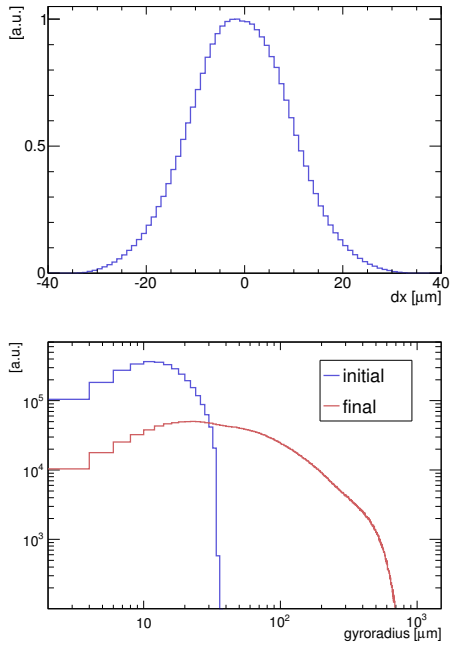

Figure 7: The position of the gyration center with respect to the position where electrons are produced (upper plot) and increase of electron gyroradii due to the beam space charge effect. The blue curve shows the gyroradius distribution for initial velocities while the red one is made after the interaction with beam space charge (6.5 TeV case).

but this effect is not affected by the bunch charge and is small (≈ 10 μm), as shown in Fig. 7.

Further investigations show (cf. Fig. 8) a strong dependence of the boosted gyroradius on the initial positions of the electrons inside the bunch. Interestingly the maximum gyroradius boost is observed for electrons produced a little closer to the bunch center than the maximum of the bunch field as shown in Fig. 9.

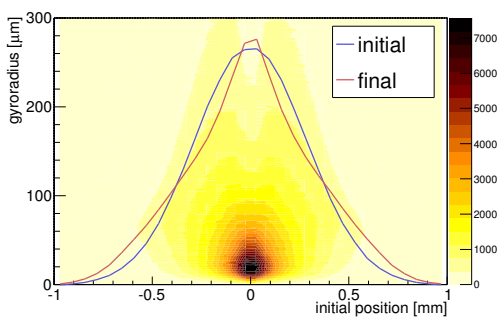

Figure 8: Increase of electron gyroradii as a function of the transverse position along the beam for 6.5 TeV case. The original and distorted beam profiles are shown, a correlation between gyroradius and transverse position is visible.

ISBN 978-3-95450-173-1

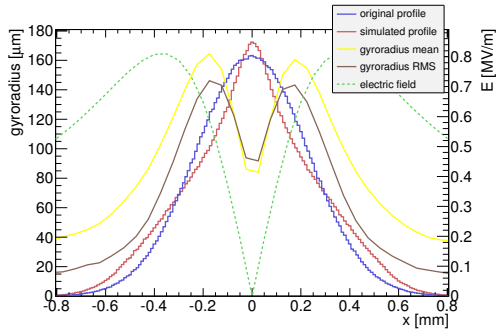

Figure 9: Correlation between gyroradius distribution properties, the bunch electric field and the beam profiles (6.5 TeV case).

PROPOSAL OF CORRECTIONS

The previous studies of corrections for the beam space charge effect were based on an iterative procedure using a set of matrices obtained with tracking simulations [9]. Here we analyze three proposals: increase of the magnetic field, use of generic properties of the distorted distributions and correction with point-spread-function depending on gyroradius.

Increase of Magnetic Field

It has been shown that an increase of the magnetic field strength to B = 1.0 T is sufficient to suppress space charge effects also for very high beam energies (see Fig. 4.11 in [5]). Here the calculations are repeated for a more realistic distribution of initial electron velocities. Figure 10 shows a comparison between the results obtained with a magnetic field strength of B = 0.2 T and B = 1.0 T. The original profile is clearly restored.

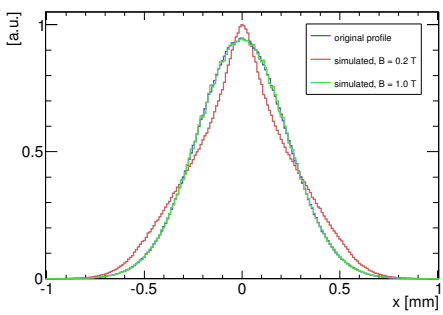

Figure 10: Comparison of distorted beam profile for B = 0.2 T and B = 1.0 T. In the latter case there is no distortion.

Interquartile Method

Because no function describing the distorted beam distribution has been found, a correlation between generic properties of a distribution and the initial beam size have been investigated. The Root Mean Square (RMS), Full Width At Half Maximum (FWHM) and Interquartile Range (Q3-Q1) have been investigated showing usually reasonable correlations and therefore giving a hope to resolve the beam size. In Fig. 11 this correlation is shown for between Q3-Q1 and the original beam size. The correlation is almost identical for all three investigated bunch intensity cases down to beam size of 0.3 mm, however for smaller beams and high bunch charges the curve becomes flat indicating the limit of this method. Similar results could be obtained using other properties of a distribution as RMS or FWHM.

The bottom plot presents that the relative blow of the emittance should still be visible, despite problems with absolute value measurement, especially if the procedure follows the accurate measurement of the beam size at injection.

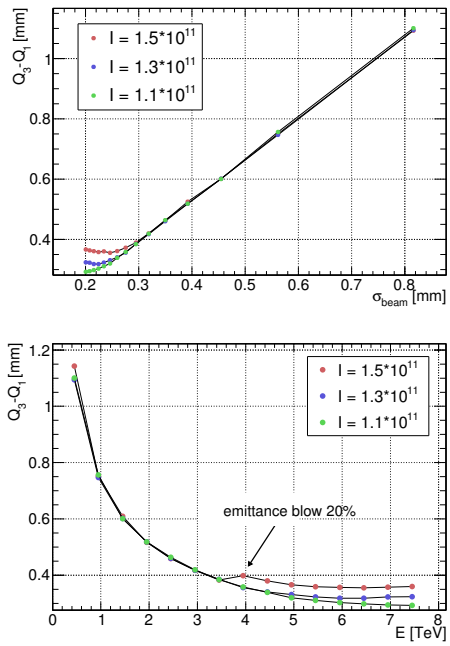

Figure 11: Upper plot: correlation between registered electron distribution interquartile range and σ_{beam} for ramps of various beam. Bottom plot: interquartile range as a function of the beam energy. For the case $N_b = 1.5 \cdot 10^{11}$ an emittance blow of 20% at 4 TeV is simulated.

Electron Sieve

The original distribution of the beam can be reconstructed if the gyroradius is known and is the same for all electrons. Fig. 12 shows the point spread function for an electron produced at x = 0 with a gyroradius of 120 μm.

The determination of the contributions to the observed profile from electrons with various gyroradii could be realized using an "electron sieve" with holes of various diameters. One should note that the sieve shall be relatively thick as the pitch of the electron helical trajectory reaches a few millimeters close to the detector.

In order to perform a deconvolution of the partial profile using the PSF from Fig. 12 a TSpectrum class from ROOT package [8] has been used. In Fig.13 a profile obtained after

ISBN 978-3-95450-173-1

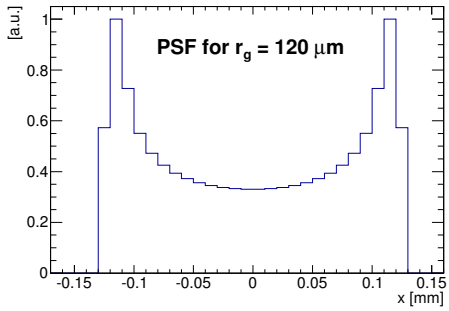

Figure 12: The distribution of the electron position at the detector for electron generated in the center and moving on helical trajectory with gyroradius 120 μm.

selecting the electrons with gyroradiuses between 100 μm and 150 is shown for 4 TeV case. The applied PSF corresponds to gyroradius of 120 μm. The deconvolution procedure recovers original shape of the two-peaked distorted profile, mainly recovers the height of the peaks as well as the depth of the central minimum. It is interesting to note that the electrons with small gyroradius (up to 75 μm) come mainly from the bunch center, while electrons with large gyroradius form characteristic double-peak distributions.

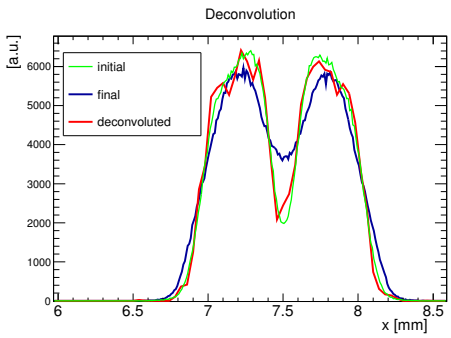

Figure 13: Deconvolution of the partial profile obtained with electrons with gyroradius between 100 and 150 μm. The PSF applied was obtained for gyroradius of 120 μm.

Fig.14 presents result of the procedure, using sieve with holes of the following diameters: 75, 100, 150 and 200 μm. For each partial profile a deconvolution procedure has been applied, using PSF obtained for gyroradii: 50, 85, 120, 170 and 200 μm respectively. The corrected profiles have been summed up and reproduce quite well the original profile.

CONCLUSIONS

In case of very high brightness LHC beams the Ionization Profile Monitors suffers from a distortion of the measured profiles due to lack of strength of the external magnetic field. The tracking simulations show a significant increase of deformation for the beam size below 0.3 mm. Observed profile shapes becomes more peaked then the initial gaussian with excess in the tails starting at about $1 - 1.5\ \sigma_{\mathrm{beam}}$ from the profile center. The average gyroradii increase from about

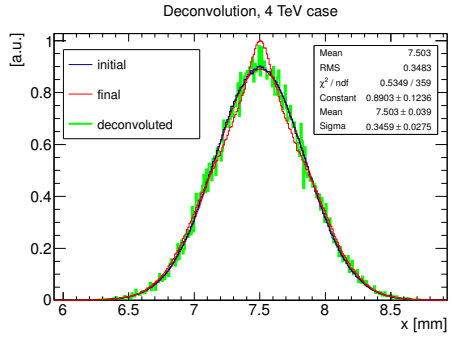

Figure 14: The result of electron sieve method.

20 μm to about 140 μm with maximum reaching 0.8 mm for 6.5 TeV beam. Attempts to fit distorted profiles with function related to the original beam width were not successful, however basic properties of the distribution, for instance interquartile range, have been found to correlate with σ_{beam}. A method based on point spread function deconvolution is being developed and the first results are promising.

ACKNOWLEDGMENT

The authors would like to thank G. Iadarola, M. Patecki and G. Francchetti for discussions and suggestions.

REFERENCES

[1] http://cern.ch/bgi

[2] M. Sapinski et al., "The First Experience with LHC Beam Gas Ionization Monitor", IBIC'12, Tsukuba, 2012, TUPB61.

[3] R. Versteegen et al., "First Proton-Nucleus Collisions in the LHC: the p-Pb pilot physics fill", CERN-ATS-2012-094 MD.

[4] G. Iadarola et al., "Electron Cloud Simulations with PyECloud", ICAP2012, Paris, 2012, WESAI4.

[5] M. Patecki, "Analysis of LHC Beam Gas Ionization monitor data and simulation of the electron transport in the detector", CERN-THESIS-2013-15.

[6] A.B. Voitkiv, N. Grun and W. Scheid, "Hydrogen and helium ionization by relativistic projectiles in collisions with small momentum transfer", J. Phys. B: At. Mol. Opt. Phys. **32** (1999) 3923-3937.

[7] M.E. Rudd, Y.-K. Kim, D.H. Madison and T.J. Gray, "Electron production in proton collisions with atoms and molecules: energy distributions", Rev. Mod. Phys. 64, 441 (1992).

[8] http://cern.ch/root

[9] J. Egberts, "IFMIF-LIPAc Beam Diagnostics: Profiling and Loss Monitoring Systems", PhD thesis CEA Saclay, 2012.

ISBN 978-3-95450-173-1